Spin-dependent avoided-crossing effect on quantum-well states in Al/W(110)

A. G. Rybkin,[1] A. M. Shikin,[1] D. Marchenko,[1,2] A. Varykhalov,[2] and O. Rader[2]
[1]*Department of Physics, St. Petersburg State University, St. Petersburg, RU-198504 Russia*
[2]*Helmholtz-Zentrum Berlin für Materialien und Energie, Elektronenspeicherring BESSY II, Albert-Einstein-Strasse 15, D-12489 Berlin, Germany*

(Received 6 June 2011; revised manuscript received 21 November 2011; published 17 January 2012)

Despite their low atomic number, Al films show large spin-orbit splittings when grown on W(110). Our spin- and angle-resolved photoemission experiment reveals two types of spin-orbit split states: quantum-well states (QWSs) with small Rashba splitting proportional to the electron wave vector in the film plane $\mathbf{k}_\parallel$ [Rashba parameter $\alpha_R \sim 7 \times 10^{-12}$ eV m for a 10-monolayer (ML) film] and substrate-derived interface states with large ($\sim$0.5-eV) splitting. The $E(\mathbf{k}_\parallel)$ dispersion of this pair of interface states changes only slightly up to 3 ML Al. At higher Al coverages, the QWSs and interface states show a remarkable avoided-crossing effect in their band dispersions. This avoided-crossing effect obeys symmetry as well as spin and, therefore, leads to a strongly enhanced spin-orbit splitting of Al QWSs. This is shown by $E(\mathbf{k}_\parallel)$ band dispersions and by spin- and angle-resolved spectra for several thicknesses up to 15 ML Al.

DOI: 10.1103/PhysRevB.85.045425 PACS number(s): 71.70.Ej, 73.20.−r, 73.21.Fg, 79.60.Dp

I. INTRODUCTION

Quantum-size effects can strongly modify the electronic structure and properties of metal films and multilayered systems.[1,2] In particular, it is well known that magnetic properties of the layered systems with alternating layers of magnetic and noble metals are strongly dependent on the thickness of the noble-metal interlayers and the quantum-size effects developing in these layers.[2–4] The thickness of the layer is the main, but not the only, important parameter for the quantization. The electronic band structure of the layer material and of the barrier material have an important influence on quantization as well. In the simple case of a single quantum film, the barriers are the interfaces to vacuum and to the substrate of the film. Intuitively, only an absolute bulk band gap in the substrate will allow for electron confinement in the quantum film. Experience shows, however, that a relative or local band gap, which exists only for a certain range of energy and electron wave vector and for a specific symmetry of the wave function, can lead to strong electron confinement, and even without any band gap, the change in atomic number at the interface gives rise to electron confinement and quantum-well states (QWSs). It has been possible to account for the simultaneous presence of these different cases in the same system by the *phase accumulation model* where the phases of the electron states, accumulated upon reflection at the interfaces, are calculated.[2,5–8] The phases of the reflected waves depend on the energy and the width of the energy band gaps in the substrate. The dependence of the QWSs on the substrate electronic structure has been investigated, at first, as a function of the film thickness, i.e., the width of the quantum well.[7–10] In these studies, the two-dimensional electron wave vector in the film plane $\mathbf{k}_\parallel$ has been kept at zero, corresponding to the center of the two-dimensional Brillouin zone and in angle-resolved photoelectron spectroscopy (ARPES) to the normal emission geometry. In this way, the influence of the substrate band gaps has been studied by ARPES for films of Ag on Cu(111) (Ref. 8) and Ni(111) (Ref. 9) and for Au on W(110).[10] For finite $\mathbf{k}_\parallel$ values out of normal emission, the influence of the substrate electronic structure can manifest itself in a change in the effective mass of electrons leading to a change in the curvature of the QWS dispersion $E(\mathbf{k}_\parallel)$.[11,12] In thin quantum films, the effective mass was found to be enhanced strongly.[11,12] Moreover, away from the Brillouin zone center, the QWS dispersions were found to suffer kinks where they enter substrate band gaps in Al/Si(111) (Ref. 13) and Ag/Ge(111).[14–17] Similar kinks and splittings near the borders of substrate band gaps were observed in Ag/Si(100),[18] Mg/W(110),[19–21] and Cu/Co(100).[22] It was pointed out that the state-crossing effect between QWSs and substrate states plays a significant role and can lead to a QWS of a certain quantum number evolving into a QWS of another quantum number.[22] Replacing the interface to vacuum by another material leads to strong changes in the quantum-well phases as well[23,24] and effects analogous to the substrate-induced modification of the QWS dispersion including kinks, which also were observed for Ag(111) layers covered by one third of a Bi monolayer.[25,26] A splitting of the quantum-well peak at the border of the substrate band gap has been observed for Ag/Ge(111) and was interpreted as a many-body effect.[27] ARPES involves final-state effects of the photoemission process. It has been pointed out that this can be avoided if, instead of a direct investigation by ARPES, a quantum film is deposited onto the material of interest and the behavior of the QWSs is studied by ARPES.[9,13] In this way, the ground state of the substrate can be restored by analysis of the QWS dispersion, which is particularly interesting when electron correlation is high, e.g., for semiconductors[13] and correlated *d* metals.[9] For Ag QWSs of 1-monolayer (ML) thickness (2 ML according to Ref. 10) on W(110), it was demonstrated that the interaction of QWSs with the substrate through the avoided-crossing effect recognizes the parity of the substrate states.[28]

The influence of the substrate also can modify the spin structure in the adsorbed film and can lead to an induced spin polarization of the formed QWSs. In particular, the induced spin polarization of QWSs at the Fermi level in noble-metal layers due to the exchange interaction in the confining ferromagnetic layers has been identified as the origin of the long-range oscillatory magnetic coupling in giant magnetoresistive spin valves.[2–4] An influence of the substrate on the spin polarization of QWSs also has been identified due to the spin-orbit interaction.[29–32] A substrate-induced spin polarization and spin-orbit splitting for noble-metal (Cu, Ag, and Au)

monolayers on the heavy-metal W(110) (Refs. 29, 30, and 32) and for noble-metal QWSs[31,32] have been shown. If only the quantum film and not the substrate has a high spin-orbit interaction, this leads to spin-polarized and spin-orbit split QWSs as well as those seen for Pb/Si(111).[33] The suggested spin-orbit splitting of QWSs in light materials (Mg) (Refs. 19 and 21) was demonstrated recently for Al/W(110), which confirms the role of the heavy-metal W as a barrier material for the spin-orbit splitting.[34] In our preliminary paper,[34] we studied the spin-orbit splitting of QWSs for 10 ML of Al/W(110) and observed a kink in the dispersion accompanied by an unexpected behavior of the spin-orbit splitting. In the present paper, we study the reasons for these effects in detail. We identify the substrate-derived states that interact in a similar way with QWSs at various film thicknesses and study, in detail, how the parabolic dispersions of the QWSs of Al/W(110) are modified when crossing the substrate-derived bands in contrast to the free-electron-like behavior. We clarify how the spin structure of the QWSs is modified by the substrate as compared with QWSs of a freestanding film and how this can be explained from the point of view of a spin-dependent avoided-crossing effect.

II. EXPERIMENTAL DETAILS

The experiments have been carried out at RGBL and UE112/PGM1 beamlines at BESSY II in ultrahigh vacuum of 1×10^{-10} to 2×10^{-10} mbar. The spin-resolved photoemission investigations were carried out using a PHOIBOS hemispherical analyzer with a Mott spin polarimeter operated at 26 kV, which is sensitive to the spin polarization in the film plane. In the present paper, data for the spin-quantization axis perpendicular to $\mathbf{k}_\parallel$ are shown. Photon energies of 62 and 65 eV were used for measurements of the valence-band photoemission spectra and of 360 and 630 eV for measurements of the W- and Al-derived core levels. The crystal structure of the W(110) surface and of the formed Al layers was determined by low-energy electron diffraction (LEED) studies. Deposition of high-purity aluminum (99.999%) on an atomically pure W(110) surface was performed at liquid-nitrogen temperature by thermal evaporation of an Al slice in a crucible of a Knudsen cell. The deposition rate of Al was controlled by a quartz microbalance, and the final thickness of deposited Al overlayers was determined by corresponding quantum-well spectra formed in the deposited Al film. The purity of the aluminum layers was controlled by the absence of oxygen core-level peaks in the photoelectron spectra and analysis of the binding energy and shape of the Al $2p$ core-level peak. The clean W(110) surface was obtained by a sharp flash up to a temperature of about 2000 °C. The details of the substrate preparation can be found in Refs. 29–32,34.

III. EXPERIMENTAL RESULTS

In Fig. 1, a series of valence-band photoemission spectra measured by angle-resolved (spin-integrated) photoemission at $h\nu = 62$ eV is shown under deposition of Al on W(110) at liquid-nitrogen temperatures. The thickness begins from submonolayer coverages and reaches 15 ML. The spectra were measured in normal emission geometry. The upper spectrum

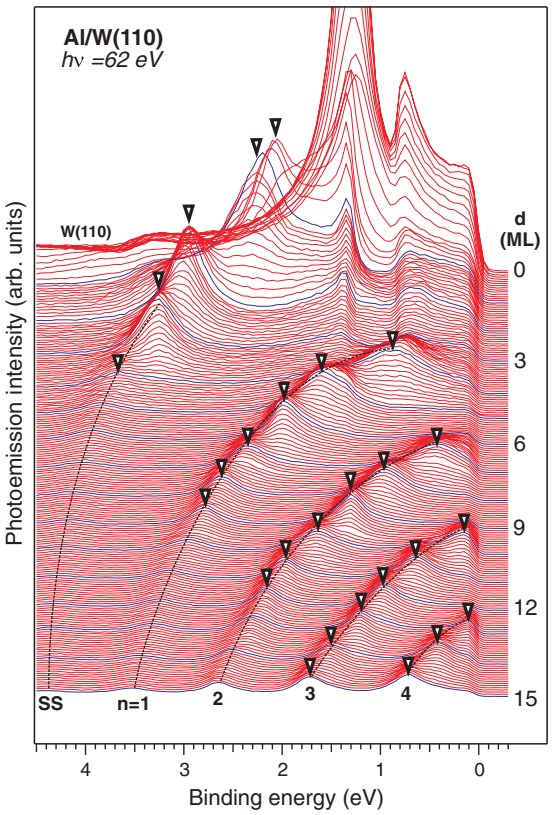

FIG. 1. (Color online) Series of ARPES (without spin resolution) measured at $h\nu = 62$ eV in normal emission geometry under deposition of Al on W(110). The thickness of the Al film is marked on the right side of the spectra. Triangles show the completion of each new Al monolayer corresponding to maximal intensities of the formed QWS peaks in the spectra.

corresponds to the pure W(110) surface. The presented spectra mainly show the thickness dependence of the QWSs formed in the depositing Al layers.

The development of the spectra is characterized by pronounced steplike changes in the energies of the QWSs, which are related to the formation of each new monolayer and by a clear separation of different QWS branches (quantum number $n = 1,2,\ldots$). In Fig. 2(a), a detailed diagram of the changes in the QWS energies with increasing Al-layer thickness is presented. The corresponding QWS intensity variations are shown in Fig. 2(c). Completion of each new monolayer corresponds to the maximal intensity of the corresponding QWS peaks. In Fig. 2(a), white and yellow colors correspond to high intensity of the formed QWS peaks. Al QWSs are formed in the entire region of the Al sp valence-band states [see Fig. 2(c)] not only in the substrate energy gap of W(110), which is located between 6.3 and 3.3 eV (Refs. 9, 10, and 20). The Al sp QWSs are shifting with increasing thickness toward the lower edge of the valence band. Branch SS (surface state) corresponds to the formation of the Al(111) surface state, which for a thick Al layer, is located at about 4.4-eV binding energy, i.e., outside of the valence band. Branch SS can be interpreted as a QWS with $n = 0$ for low thicknesses, which is transforming with the deposition of Al into the Al surface state located, for the (111) surface of bulk Al, at about 4.68 eV.[13,35] In Fig. 2(b), for comparison, the $E(\mathbf{k}_\parallel)$ dispersion dependence

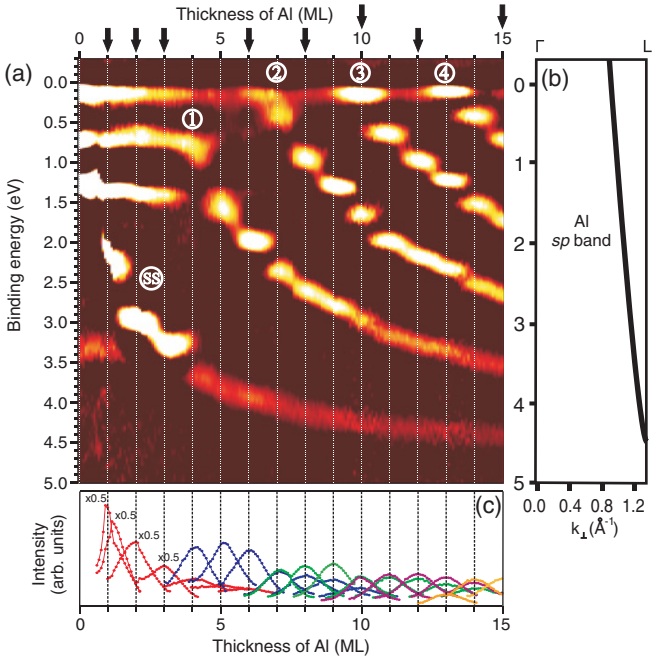

FIG. 2. (Color online) (a) Dependence of QWS energies in normal emission with thickness under deposition of Al on W(110). The diagram displays the second derivative of the photoemission intensity also shown in Fig. 1, with the white color corresponding to maximum and the black color corresponding to minimum values. The labels 1–4 indicate branches of QWSs. Arrows indicate the thicknesses for which dispersion dependences and spin-resolved spectra have been measured (see Figs. 3–7). (b) Dispersion of the Al-bulk *sp* states in the growth direction of the film (Ref. 39). (c) Photoemission intensities of selected QWSs used for a precise thickness calibration.

of Al *sp* states in the growth direction of the Al film shows the possible energy region of the Al *sp* QWS formation. Discrete QWS energy values characteristic of each monolayer and the linear increase in QWS intensities with increasing thicknesses have been used in the present paper for the precise calibration of the thicknesses of the investigated Al films. To confirm the reliability of the calibration, the thickness of the formed layers has been tested earlier using the attenuation of the W $4f_{7/2}$ peak intensity.[36] The character of the changes in the QWS spectra with the thickness testifies to the layer-by-layer growth of Al films on W(110). It should be noted that the substrate was cooled down before deposition to prevent formation of islands, which at room temperature, takes place above a 3-ML thickness. In Figs. 3(a)–3(d), the changes in the LEED pattern for different thicknesses of the deposited Al are shown. Clearly, it is seen that pseudomorphous layers of Al are formed up to 3-ML thicknesses, while higher thicknesses lead to a Kurdjumov-Sachs orientation.[37,38] The surface Brillouin zone of W(110) with high-symmetry directions is shown in Fig. 3(e) by dashed lines. Additionally, Brillouin zones of two Al domains display the rotation of Al domains relative to the W substrate for this growth mode.

Figure 4 shows the dispersion dependences $E(\mathbf{k}_\parallel)$ of the quantum and interface states formed under deposition of Al on W(110), which were measured in the $\bar{\Gamma}\bar{S}$ direction of the surface Brillouin zone for different thicknesses up to 15 ML of

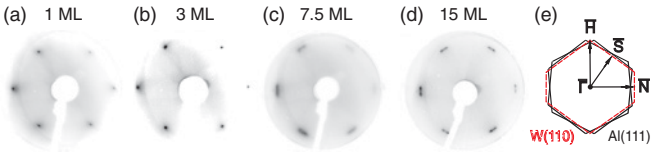

FIG. 3. (Color online) LEED patterns of Al layers on W(110) for different thicknesses: (a) 1 ML, (b) 3 MLs, (c) 7.5 MLs, and (d) 15 MLs. The energy of the incident electron beam is (a) and (b) 98 eV and (c) and (d) 73 eV. (e) Surface Brillouin zone of W(110) and of two Al domains with Kurdjumov-Sachs orientation.

Al. (The thicknesses of the films for which dispersions of the QWSs were measured were marked in the upper part of Fig. 2 by black arrows). In Fig. 4(a), the corresponding dispersions for pure W(110) are shown for comparison. The edges of the (110)-projected bulk energy gap in W are marked by dotted lines.[39]

The dispersions for pure W(110) are characterized by W 5*d* surface resonances[40] located for normal emission (i.e., 0°) at binding energies of about 0.7 and 1.2 eV, which disperse only up to the border of the W surface-projected energy gap. It is interesting that, in the region near 1.2-eV binding energy close to normal emission, two almost linear dispersions along $\bar{\Gamma}\bar{S}$ intersect, which are reminiscent of massless Dirac fermions. A more detailed study of their behavior will be published elsewhere. After deposition of 1 to 2 monolayers of Al these states are transforming into Al-W interface states that already are extending into the region of the W-derived energy gap [see blue line in Fig. 4(b)].

The resulting interface states marked as $I^{|}$ and $I^{||}$ have maximal intensity in the region of the W-derived surface-projected energy gap. The states almost become nondispersing keeping their splitting throughout the W gap. The intensities of these photoemission features are maximal in the region of the W-energy gap. In addition, at 2-ML thicknesses, the Al QWS with $n = 0$ is formed. For thicker Al, this state transforms into the state marked SS. It is located at about a 3-eV binding energy at normal emission and has paraboliclike dispersion with kinks where it crosses the region of the W 6*p* states (see further below).

An increase from 2 [Fig. 4(b)] to 3 ML Al [Fig. 4(c)] does not lead to strong modification in the dispersions of the interface and QW states. They are very similar to those observed at 2 ML Al, however, with some energy shift in SS (to about 3.2 eV) and minor modification of the interface states in the W-derived energy gap.

The interface states for 3 MLs of Al also are marked here as $I^{|}$ and $I^{||}$. They clearly are visible and are marked by red and blue lines for comparison with other dispersions presented in Fig. 4. As noted above, these states are W-derived states and are formed due to hybridization between electronic states of the W surface and the deposited Al and are localized at the interface. At 3-ML thickness, an intersection between dispersions of the interface ($I^{|}$,$I^{||}$) and SS states does not take place, and they do not influence each other. The interface states are transforming under deposition of the second and third Al atom layers, which still influence the bonds at the interface. After completion of 3 monolayers, these states are stabilized, and further deposition

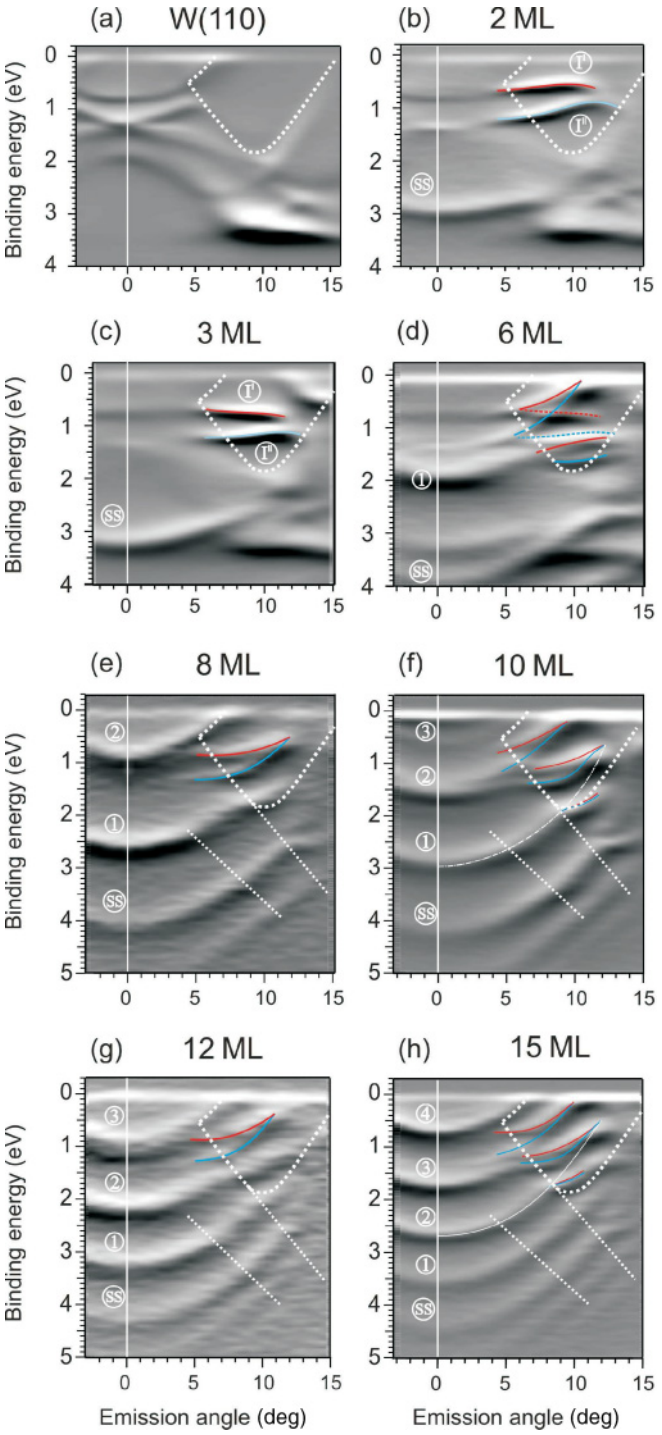

FIG. 4. (Color) Angle-resolved photoemission data at (a) $h\nu$ = 65 eV and (b)–(h) 62 eV as a function of binding energy and emission angle for (a) a pure W(110) surface and (b)–(h) for 2–15 ML of Al on W(110). The labels $I^{|}$ and $I^{||}$ indicate interface states formed at thicknesses of 2 and 3 ML. The label SS corresponds to an Al(111)-derived surface state, and labels from 1 to 4 correspond to QWSs. The data are presented in the form of the first derivative of the photoemission spectra. The borders of the W surface-projected energy gap are marked by dotted lines, and expected W 6p dispersions are marked by two straight dotted lines. The interaction with the interface states is marked in blue for spin up and red for spin down as gathered from spin-resolved data (Figs. 5–7).

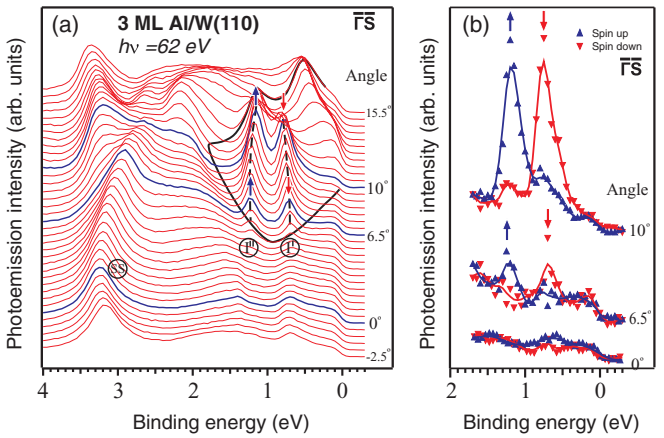

FIG. 5. (Color online) Series of (a) angle-resolved spin-integrated and (b) spin-resolved photoemission spectra for varying off-normal polar angles for 3 ML Al on W(110). States of different spins are distinguished by blue and red symbols and corresponding arrows. The labels $I^{|}$ and $I^{||}$ indicate the interface states, and SS indicates the Al(111)-derived surface state. Blue lines in (a) correspond to the polar angles for which the spin-resolved spectra were measured in (b). A thin black line shows the borders of the W surface-projected energy gap.

of Al does not lead to principal changes in their energy and splitting.

For analysis of the spin structure of the split interface states, we have measured the corresponding spin-resolved photoemission spectra for 3 MLs and higher thicknesses of the Al overlayer. In Figs. 5(a) and 5(b), the corresponding series of angle-resolved spin-integrated and spin-resolved photoemission spectra are shown for different polar angles relative to the surface normal. The values of the polar angle are shown on the right side from the presented spectra.

The spin-integrated photoemission spectra that correspond to the spin-resolved spectra in Fig. 5(b) are marked in Fig. 5(a) by thick blue lines. Figure 5(b) shows that the interface states $I^{|}$ and $I^{||}$ practically are fully spin polarized. Corresponding spin orientations are in accordance with the Rashba model and are shown in Figs. 5(a) and 5(b) by red and blue symbols and corresponding arrows. The region of the W-derived energy gap is shown by thin black lines. The presented spin-resolved spectra indicate the spin polarization of the interface states and enable the precise determination of their energies.

The next dispersions shown in Fig. 4(d) correspond to 6-ML thickness. For this thickness, an additional QWS is formed at a binding energy of 1.8 eV for normal emission (see, for comparison, Fig. 2), which is marked as (1). Branch SS is located at a binding energy of 4.0 eV. The QWS dispersion (1) intersects at this Al thickness the dispersions of spin-polarized interface states ($I^{|}$,$I^{||}$). As a result, a complex picture of interacting and mixed dispersions is observed. In Fig. 6, the series of corresponding angle-integrated [Fig. 6(a)] and spin-resolved [Fig. 6(b)] photoemission spectra are shown for detailed analysis. The positions of the interface states ($I^{|}$,$I^{||}$) are shown by dotted lines. The states are marked by red and blue symbols for the spin and corresponding arrows. When the dispersion of the QWS No. 1 intersects the interface states ($I^{|}$ and $I^{||}$), a significant modification of the dispersions takes place.

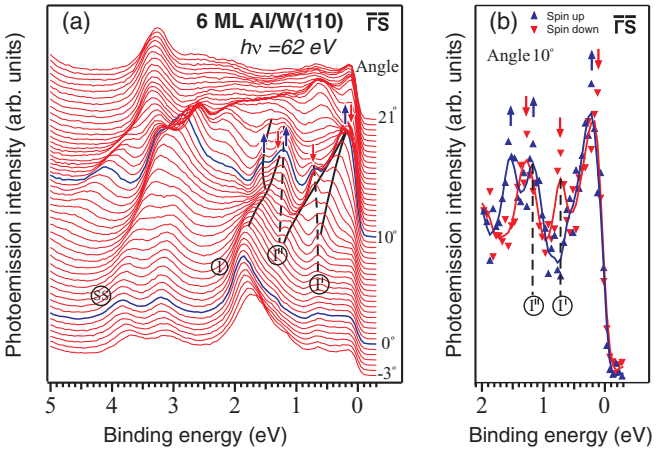

FIG. 6. (Color online) Same as Fig. 5 but for 6 ML Al. Label 1 marks the QWS. Black thin lines show dispersions of QWSs split into two with different spin orientations.

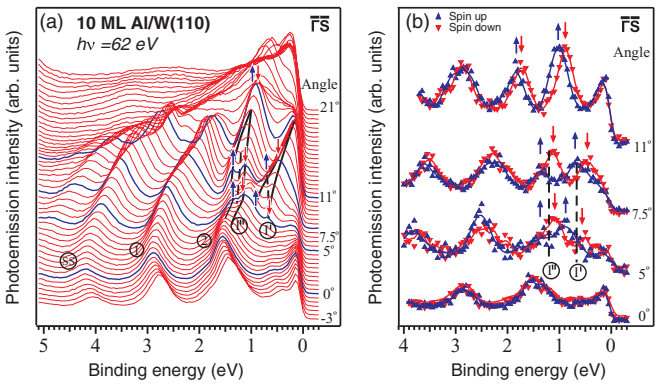

FIG. 7. (Color online) Same as Figs. 5 and 6 but for 10 ML Al.

The QWS dispersion is split into two parts with different spin orientations. Therefore, each part of the QWS interacts with the interface states with the same spin. In the intersection region of the QWS and the pronounced spin-polarized interface states, an avoided-crossing effect takes place, which breaks the parabolic dispersion of the QWS. A sketch of such spin-dependent avoided-crossing effects can be seen in the left part of Fig. 9 similar to the QWS No. 2 presented in the figure. As shown in this scheme, a significant spin splitting occurs at the assumed intersection. In the regions far from this intersection, the spin splitting is significantly smaller, and the dispersions of QWSs appear unaffected by the avoided-crossing effect.

The next characteristic modification in the dispersions of the Al QW states is shown in Fig. 4(e) and takes place at 8-ML thickness. For this thickness, we already observe two QWSs in the analyzed energy region (marked as 1 and 2) at energies of about 2.7 and 0.9 eV for normal emission (see, for comparison, the energies of the QWSs in Fig. 2). For these thicknesses, the interface states appear in the region between dispersions of QWSs. Only QWS No. 1 intersects the interface states ($I^{|}$ and $I^{||}$) in the k-space region where they cease to exist. The interaction between the spin-polarized interface and the QWSs again leads to an avoided-crossing effect and corresponding spin splitting of the QWS. However, the manifestation of the spin-polarized avoided-crossing effect differs from the previous case. Outside of the k-space region of localization of the interface states (for polar angles $>10°$ off-normal), the spin splitting of the QWS branch already is reduced significantly as compared to the one in the region of the projected W gap.

For a thickness of 10 ML [Fig. 4(f)], two QWSs are located already in the region of the intersection with the interface states inside of the W energy gap. In Fig. 7, the corresponding series of (a) spin-integrated and (b) spin-resolved photoemission spectra is shown for different polar angles relative to the surface normal. The positions of the interface states also are shown by dotted lines. The states characterized by different spins also are marked by red and blue symbols and corresponding arrows. Again, the spin-polarized states from each QWS interact with the spin-polarized interface states with the same spin. It results in a series of spin-polarized dispersions in the region of the assumed intersection caused by the spin-dependent avoided-crossing effect. A sketch of the modification of the dispersion of the states with different directions of spin is shown in Fig. 9. In this case, the spin-dependent avoided-crossing interaction has to lead to the formation of a characteristic loop of the dispersions that, indeed, can be distinguished in Fig. 4(d).

Concerning the QWSs observed at about 2.8 and 4.1 eV, which are marked in Figs. 4(f) and Fig. 7(a) as (1) and (SS), respectively, we cannot distinguish any well-defined splitting by spin-integrated photoemission. On the other hand, by analyzing spin-resolved spectra in Fig. 7(b), we can distinguish a spin splitting of the QWS, for instance, for branch (1). By analyzing the splitting value for this branch, we can see the tendency of increasing splitting with increasing $\mathbf{k}_{\parallel}$. This behavior is similar to that observed for the QWSs in Au and Ag layers on W(110) (Refs. 31 and 32), which can be described in the framework of the Rashba model for a two-dimensional electron gas modified by inclusion of the substrate.[41,42] We can quantify the strength of the Rashba effect at 10 ML Al/W(110) from the QWS with $n = 1$ in Fig. 7 by the Rashba parameter $\alpha_R \sim 7 \times 10^{-12}$ eV m. This is somewhat less than the effect on the surface state of Au(111) ($\sim 3.3 \times 10^{-11}$ eV m) (Ref. 43) and the $n = 1$ QWS in 5 ML Au/W(110) ($\sim 1.6 \times 10^{-11}$ eV m).[31]

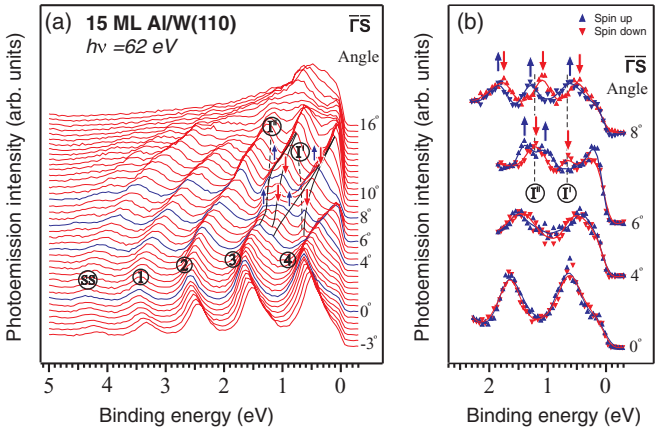

FIG. 8. (Color online) Same as Figs. 5–7 but for 15 ML Al.

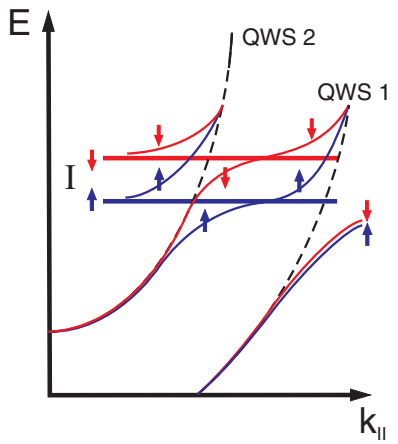

FIG. 9. (Color online) Sketch based on spin-resolved experimental data. Spin-dependent dispersions are modified under an intersection with spin-split interface states. Here, the crossing of the spin-split interface states by two QWSs is shown.

For a thickness of 12 ML [Fig. 4(g)], the features and scheme of the avoided-crossing interaction, to some degree, are similar to the situation taking place for the 8-ML thickness. The region of the spin-polarized interface states is located in k space between the QWS dispersions. As a result of the avoided-crossing effect, a fork of the hybrid spin-split states is formed, which is similar to that observed for 8 MLs of Al. In this case, a pronounced spin splitting clearly is observed where the QWS No. 2 crosses the interface states (for polar off-normal angles $<10^\circ$) and significantly reduced spin splitting away from the crossing (for polar off-normal angles $>10^\circ$). For a thickness of 15 ML, two QWSs intersect the interface states [Fig. 4(h)]. As a result, we can see the formation of, at least, three pronounced bended dispersions already by spin-integrated photoemission [Fig. 8(a)] and four clearly visible spin-polarized branches in the region of the W-derived energy gap [Fig. 8(b)]. This is the situation again sketched in Fig. 9.

Under the intersection of QWSs with W $6p$ states (dispersions are shown in Fig. 4 by dotted lines in the energy region between 2 and 4 eV) some bending and jumps of the QWS dispersions also are observed. However, in this case, the modification of the dispersions is less dramatic. Moreover, a large spin polarization of QWSs in this region is not observed. Only some peak broadening and bending of the dispersion in the intersection region are observed. These modifications can be described as closer to the cases reported for Al/Si(111) (Ref. 13), Ag/Si(100) (Ref. 18), and Ag/Ge(111).[16,17,27]

IV. CONCLUSION

We observe very strong modifications in the dispersion of Al s,p-derived QWSs in Al (111) films on W(110). Some of these are spin polarized strongly with large spin-orbit splittings unexpected for Al with its small nuclear charge of 13. By detailed investigations of various thicknesses, we could distinguish between a low-thickness range ($\leqslant$3 MLs) and a high-thickness range (4–15 MLs). The low-thickness range allows for the observation of states with a very large ($\sim$0.5 eV) spin-orbit splitting independent of $\mathbf{k}_\parallel$. They appear inside a (110)-projected bulk band gap of W and are assigned to Al-W interface states that have their origin in the surface electronic structure of W(110). The high-thickness range shows QWSs inside and outside of the (110)-projected bulk band gap of the W substrate with increased two-dimensional confinement and enhanced photoemission intensity inside of the gap. When the $E(\mathbf{k}_\parallel)$ dispersions of these QWSs cross the dispersions of the interface states, they interact in the intersection region. The interaction leads to the formation of hybrid bonding and antibonding states located at higher- and lower-binding energies than the expected intersection and the opening of a corresponding local energy gap. It is shown that each state interacts with the state of the same spin. Because the interacting interface states are initially spin polarized with large spin-orbit splitting, the resulting bonding and antibonding states differ for each spin orientation. Where two dispersions of QWSs intersect the interface states, the spin-dependent avoided-crossing effect leads to the formation of a characteristic loop of spin-split hybrid states.

The observed spin-dependent avoided-crossing effect has a general character characteristic of any system where states with pronounced spin splitting intersect those of weaker splitting. In this way, a large spin-orbit splitting is transferred to light atoms, such as Al even when these atoms are in a quantum film several interatomic distances away from the heavy element.

ACKNOWLEDGMENTS

This work was supported by DFG-RFBR projects (Projects No. 11-02-91337, No. 11-02-91344, and No. RA 1041/3-1), RFBR project (Project No. 11-02-00642-a) and a grant from St. Petersburg State University for scientific investigations. Some of the authors (A.G.R. and A.M.S.) acknowledge support from the Russian-German laboratory at BESSY II.

[1]T.-C. Chiang, Surf. Sci. Rep. **39**, 181 (2000).
[2]F. J. Himpsel, J. E. Ortega, G. J. Mankey, and R. F. Willis, Adv. Phys. **47**, 511 (1998).
[3]C. Carbone, E. Vescovo, O. Rader, W. Gudat, and W. Eberhardt, Phys. Rev. Lett. **71**, 2805 (1993); K. Garrison, Y. Chang, and P. D. Johnson, *ibid.* **71**, 2801 (1993); J. E. Ortega and F. J. Himpsel, *ibid.* **69**, 844 (1992).
[4]P. D. Johnson, Rep. Prog. Phys. **60**, 1217 (1997).
[5]S. Å. Lindgren and L. Walldén, Phys. Rev. Lett. **59**, 3003 (1987).
[6]N. V. Smith, N. B. Brookes, Y. Chang, and P. D. Johnson, Phys. Rev. B **49**, 332 (1994).
[7]S. Å. Lindgren and L. Walldén, Phys. Rev. Lett. **61**, 2894 (1988).
[8]M. A. Mueller, A. Samsavar, T. Miller, and T.-C. Chiang, Phys. Rev. B **40**, R5845 (1989).
[9]A. Varykhalov, A. M. Shikin, W. Gudat, P. Moras, C. Grazioli, C. Carbone, and O. Rader, Phys. Rev. Lett. **95**, 247601 (2005).
[10]A. M. Shikin, O. Rader, G. V. Prudnikova, V. K. Adamchuk, and W. Gudat, Phys. Rev. B **65**, 075403 (2002).

[11]C. Carbone, E. Vescovo, R. Kläsges, W. Eberhardt, O. Rader, and W. Gudat, J. Appl. Phys. **76**, 6966 (1994).
[12]P. D. Johnson, K. Garrison, Q. Dong, N. V. Smith, D. Li, J. Mattson, J. Pearson, and S. D. Bader, Phys. Rev. B **50**, R8954 (1994).
[13]L. Aballe, C. Rogero, P. Kratzer, S. Gokhale, and K. Horn, Phys. Rev. Lett. **87**, 156801 (2001).
[14]S.-J. Tang, Y.-R. Lee, S.-L. Chang, T. Miller, and T.-C. Chiang, Phys. Rev. Lett. **96**, 216803 (2006).
[15]P. Moras, L. Ferrari, C. Spezzani, S. Gardonio, M. Ležaić, Ph. Mavropoulos, S. Blügel, and C. Carbone, Phys. Rev. Lett. **97**, 206802 (2006).
[16]S.-J. Tang, T. Miller, and T.-C. Chiang, Phys. Rev. Lett. **96**, 036802 (2006).
[17]P. Moras, D. Topwal, P. M. Sheverdyaeva, L. Ferrari, J. Fujii, G. Bihlmayer, S. Blügel, and C. Carbone, Phys. Rev. B **80**, 205418 (2009).
[18]I. Matsuda, T. Ohta, and H. W. Yeom, Phys. Rev. B **65**, 085327 (2002).
[19]F. Schiller, R. Keyling, E. V. Chulkov, and J. E. Ortega, Phys. Rev. Lett. **95**, 126402 (2005).
[20]A. M. Shikin and O. Rader, Phys. Rev. B **76**, 073407 (2007).
[21]C. Koitzsch, C. Battaglia, F. Clerc, L. Despont, M. G. Garnier, and P. Aebi, Phys. Rev. Lett. **95**, 126401 (2005).
[22]E. Rotenberg, Y. Z. Wu, J. M. An, M. A. Van Hove, A. Canning, L. W. Wang, and Z. Q. Qiu, Phys. Rev. B **73**, 075426 (2006).
[23]F. J. Himpsel and O. Rader, Appl. Phys. Lett. **67**, 1151 (1995).
[24]A. M. Shikin, D. V. Vyalikh, Yu. S. Dedkov, G. V. Prudnikova, V. K. Adamchuk, E. Weschke, and G. Kaindl, Phys. Rev. B **62**, R2303 (2000).
[25]K. He, T. Hirahara, T. Okuda, S. Hasegawa, A. Kakizaki, and I. Matsuda, Phys. Rev. Lett. **101**, 107604 (2008).
[26]E. Frantzeskakis, S. Pons, H. Mirhosseini, J. Henk, C. R. Ast, and M. Grioni, Phys. Rev. Lett. **101**, 196805 (2008).
[27]S.-J. Tang, L. Basile, T. Miller, and T.-C. Chiang, Phys. Rev. Lett. **93**, 216804 (2004).
[28]D. V. Vyalikh, Yu. Kucherenko, F. Schiller, M. Holder, A. Kade, S. L. Molodtsov, and C. Laubschat, Phys. Rev. B **76**, 153406 (2007).
[29]A. M. Shikin, A. Varykhalov, G. V. Prudnikova, D. Usachov, V. K. Adamchuk, Y. Yamada, J. D. Riley, and O. Rader, Phys. Rev. Lett. **100**, 057601 (2008).
[30]A. M. Shikin, A. Varykhalov, O. Rader, V. K. Adamchuk, and W. Gudat, Appl. Phys. A **94**, 449 (2009).
[31]A. Varykhalov, J. Sánchez-Barriga, A. M. Shikin, W. Gudat, W. Eberhardt, and O. Rader, Phys. Rev. Lett. **101**, 256601 (2008).
[32]A. M. Shikin, A. G. Rybkin, D. E. Marchenko, D. U. Usachov, V. K. Adamchuk, A. Varykhalov, and O. Rader, Phys. Solid State **52**, 1515 (2010).
[33]J. H. Dil, F. Meier, J. Lobo-Checa, L. Patthey, G. Bihlmayer, and J. Osterwalder, Phys. Rev. Lett. **101**, 266802 (2008).
[34]A. G. Rybkin, A. M. Shikin, V. K. Adamchuk, D. Marchenko, C. Biswas, A. Varykhalov, and O. Rader, Phys. Rev. B **82**, 233403 (2010).
[35]L. Aballe, C. Rogero, S. Gokhale, S. Kulkarni, and K. Horn, Surf. Sci. **482-485**, 488 (2001).
[36]A. G. Rybkin, D. Y. Usachov, D. E. Marchenko, A. M. Shikin, V. K. Adamchuk, A. Y. Varykhalov, and O. Rader, Surf. Invest. X-ray Synchrotron Neutron Tech. **4**, 401 (2010).
[37]G. Kurdjumov and G. Sachs, Z. Phys. **64**, 325 (1930).
[38]O. Hellwig, K. Theis-Bröhl, G. Wihelmi, and H. Zabel, Surf. Sci. **410**, 362 (1998).
[39]D. A. Papaconstantopoulos, *Handbook of the Band Structure of Elemental Solids* (Plenum, New York, 1986).
[40]R. H. Gaylord and S. D. Kevan, Phys. Rev. B **36**, 9337 (1987).
[41]E. I. Rashba, Fiz. Tverd. Tela (Leningrad) **2**, 1224 (1960) [Sov. Phys. Solid State **2**, 1109 (1960)].
[42]L. Petersen and P. Hedegård, Surf. Sci. **459**, 49 (2000).
[43]H. Cercellier, C. Didiot, Y. Fagot-Revurat, B. Kierren, L. Moreau, D. Malterre, and F. Reinert, Phys. Rev. B **73**, 195413 (2006).